DEUTSCHES ELEKTRONEN-SYNCHROTRON **DESY**

DESY 84-048
June 1984

WEAK INTERACTIONS

PETRA RESULTS

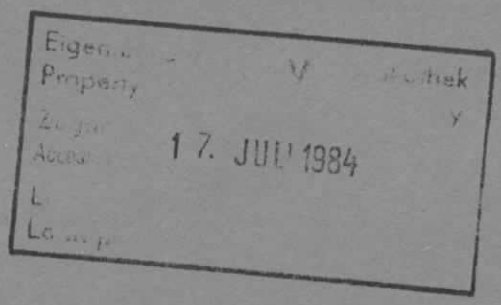

by

H.-U. Martyn

I. Physikalisches Institut der RWTH, Aachen

ISSN 0418-9833

NOTKESTRASSE 85 · 2 HAMBURG 52

To be sure that your preprints are promptly included in the
HIGH ENERGY PHYSICS INDEX ,
send them to the following address (if possible by air mail) :

DESY
Bibliothek
Notkestrasse 85
2 Hamburg 52
Germany

DESY 84-048
June 1984

ISSN 0418-9833

Weak Interactions
PETRA Results

HANS-ULRICH MARTYN[1]

I. Physikalisches Institut der RWTH, Aachen, Germany

ABSTRACT. Recent results on weak interactions from experiments at the PETRA e^+e^- storage ring are presented. They include the determination of the weak neutral couplings in the purely leptonic reactions $e^+e^- \to e^+e^-$, $e^+e^- \to \mu^+\mu^-$ and $e^+e^- \to \tau^+\tau^-$ and in the production of heavy charm and bottom quarks $e^+e^- \to c\,\bar{c}$ and $e^+e^- \to b\,\bar{b}$. The weak charged current is tested in τ decays, where new data on semihadronic branching ratios and a new lifetime measurement is reported, and in semileptonic decays of charm and bottom quarks.

1. Introduction.

e^+e^- storage rings offer a unique possibility to study the weak interactions of leptons and quarks. Teir production is dominated by the electromagnetic interaction, however, at PETRA / PEP energies the interference between the electromagnetic (photon exchange) and the weak (Z^0 exchange) amplitudes leads to measurable effects. Weak neutral current couplings can be measured in purely leptonic reactions, which may be compared with results from νe scattering experiments at low space like momentum transfer, and for the abundantly produced heavy charm and bottom quarks via the reaction $e^+e^- \to q\bar{q} \to hadrons$. The dynamics of the weak current can be can be studied via the decays of e. g. τ leptons and charm and bottom quarks.

The main goal is to provide further tests of the standard theory of Glashow, Weinberg and Salam[1)] (GWS), complementing neutrino electron and lepton nucleon scattering experiments[2)] and the recent discoveries of the W and Z^0 bosons[3)].

In this talk recent results will be reported on

- electroweak interference in the leptonic reactions $e^+e^- \to e^+e^-$, $e^+e^- \to \mu^+\mu^-$ and $e^+e^- \to \tau^+\tau^-$,
- production and decays of heavy quarks $e^+e^- \to c\,\bar{c}$ and $e^+e^- \to b\,\bar{b}$,
- charged currents in τ decays: new branching ratios and a lifetime measurement.

The data come from the PETRA experiments Cello, Jade, Mark J, Pluto and Tasso. Most data ($\sim 70\ pb^{-1}$ per experiment) have been accumulated at an average cm energy of 34.5 GeV. Some recent results ($\sim 12\ pb^{-1}$ per experiment)from an energy scan between 40 and 46 GeV are included. In the near future much more data from PETRA running at the highest energy of ~45 GeV will be expected.

2. Neutral Current Formalism.

The differential cross section for the production of a fermion antifermion pair $e^+e^- \to f\,\bar{f}$ (with f = μ, τ or q ; if f = e the t-channel diagrams have to be included) is given by[4)]

$$\frac{d\sigma}{d\Omega} = \frac{\alpha^2}{4\,s} \cdot \left\{ F_1(s)\ (1 + \cos^2\theta) + 2\,F_3(s)\ \cos\theta \right\} \quad . \tag{1}$$

[1]Invited talk given at the Symposium on High Energy e^+e^- Interactions, Vanderbilt University,Nashville, April 5 - 7, 1984

Here $\sqrt{s} = W$ is the center of mass energy and θ is the polar scattering angle measured between the incoming and the outgoing particle. The coefficients

$$F_1(s) = Q_f^2 - 2Q_f\, Re(\chi)\, g_V^e\, g_V^f + |\chi|^2\, (g_A^{e2} + g_V^{e2})(g_A^{f2} + g_V^{f2}) \tag{2a}$$

$$F_3(s) = \quad -2Q_f\, Re(\chi)\, g_A^e\, g_A^f + 4\,|\chi|^2\, g_A^e\, g_V^e\, g_A^f\, g_V^f \tag{2b}$$

are given in $SU(2)_L \times U(1)$ models in terms of the fermion charge Q_f, the weak vector coupling $g_V^f = I_{3L} - 2\, Q_f\, \sin^2\theta_W$, the weak axial vector coupling $g_A^f = I_{3L}$ ($I_L = \frac{1}{2}$ being the left handed weak isospin) and a Z^0 propagator including the overall weak neutral current strength $\sin^2\theta_W$

$$\chi = \frac{1}{4\, \sin^2\theta_W\, \cos^2\theta_W} \cdot \frac{s}{s - m_Z^2 + i m_Z \Gamma} \tag{3a}$$

$$= \frac{\rho\, G_F\, m_Z^2}{2\sqrt{2}\,\pi\,\alpha} \cdot \frac{s}{s - m_Z^2 + i m_Z \Gamma} \quad . \tag{3b}$$

m_Z and Γ are the mass and width of the Z^0 boson, $G_F = 1.166 \cdot 10^{-5}\ GeV^{-2}$ is the Fermi constant. Eq. (3b) is derived from eq. (3a) by relating the strength of the neutral current and the charged current through

$$\rho = \frac{m_W^2}{m_Z^2\, \cos^2\theta_W} \,. \tag{4}$$

In the GWS theory with one Higgs doublet we have $\rho = 1$ and are left with the only free parameter $\sin^2\theta_W$. Taking $\sin^2\theta_W = 0.228 \pm 0.010$ from neutrino nucleon scattering experiments[13] (neglecting radiative corrections) the coupling constants of the standard theory are summarised in Table 1.

Table 1. Electroweak coupling constants for fermions in the standard theory

fermion	Q_f	g_A^f	g_V^f	g_V^f $(\sin^2\theta_W = 0.228)$
leptons e^-, μ^-, τ^-	-1	$-\frac{1}{2}$	$-\frac{1}{2} + 2\sin^2\theta_W$	-0.044
quarks u , c	$+\frac{2}{3}$	$+\frac{1}{2}$	$+\frac{1}{2} - \frac{4}{3}\sin^2\theta_W$	$+0.196$
quarks d , s , b	$-\frac{1}{3}$	$-\frac{1}{2}$	$-\frac{1}{2} + \frac{2}{3}\sin^2\theta_W$	-0.348

The total cross section normalised to the pointlike QED cross section $\sigma_{pt} = 4\pi\alpha^2/3s$ is given by

$$R_{f\bar{f}} = F_1(s) \,. \tag{5}$$

It is sensitive to the vector couplings, but since $g_V^e \sim 0$ no appreciable interference effect is measurable. For μ pair production the increase between 34.5 GeV and 45 GeV is $\Delta R_{\mu\mu} = 1.4\%$. For hadron production eq. (5) has to be multiplied by a colour factor of 3 and QCD terms $(1 + \alpha_s/\pi + \ldots) \sim 1.05$. The net increase due to electroweak interference is $\Delta R_{had} = 5.6\%$ from 34.5 GeV to 45 GeV, a number comparable to the typical experimental uncertainties. The measurements only allow to restrict the range of $\sin^2\theta_W$, e.g. $\sin^2\theta_W = 0.27 \pm 0.06$ (Jade[5]).

The forward-backward asymmetry in the interference region is defined by

$$A_{f\bar{f}} = \frac{N_F - N_B}{N_F + N_B} = \frac{3}{4}\frac{F_3}{F_1} \simeq \frac{3}{2}\frac{g_A^e\, g_A^f}{Q_f}\, Re(\chi) \,, \tag{6}$$

where N_F is the number of forward going ($\cos\theta > 0$) and N_B is the number of backward going ($\cos\theta < 0$) fermions. It measures the axial vector couplings of the fermions and is considerably larger for quarks than for leptons. This asymmetry is substantial, in particular at the highest PETRA energies. The predicted values are $A_{\mu,\tau}(34.5\ GeV) = -9.3\%$ and $A_{\mu,\tau}(45\ GeV) = -17.8\%$ for lepton production, $A_u(34.5\ GeV) = -14\%$ and $A_u(45\ GeV) = -27\%$ for up type quarks and $A_d(34.5\ GeV) = -28\%$ and $A_d(45\ GeV) = -39\%$ for down type quarks.

3. Electroweak interference in leptonic reactions.

3.1. $e^+e^- \to e^+e^-$.

Bhabha scattering $e^+e^- \to e^+e^-$ has been studied by the PETRA experiments[6] with high statistics at $\sqrt{s} \simeq 34.5$ GeV and with moderate statistics at $\sqrt{s} \simeq 42.5$ GeV. The differential cross section corrected for order α^3 QED radiative effects[7] and normalised to the QED prediction is shown for the Tasso experiment in Fig. 1.

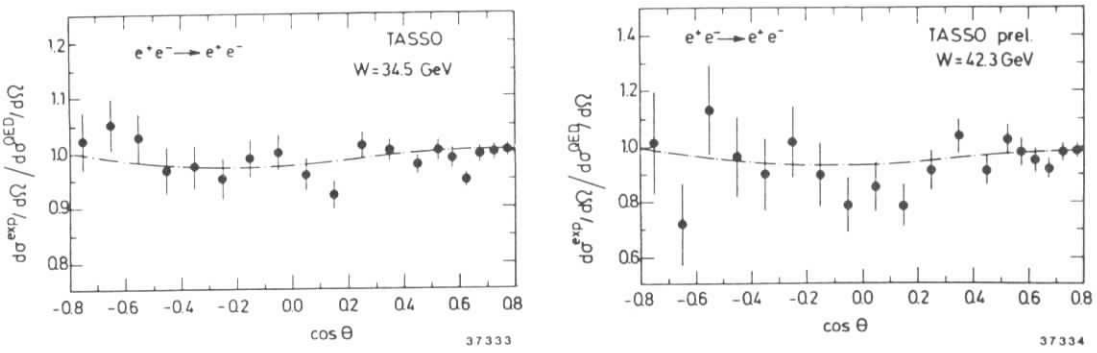

Figure 1. The differential cross section normalised to the QED prediction for the reaction $e^+e^- \to e^+e^-$ at a) $\sqrt{s} = 34.5\ GeV$ and b) $\sqrt{s} = 42.3\ GeV$ from Tasso. The curves are fits to the standard theory with $\sin^2\theta_W = 0.26$.

The data are well described by QED. They are also compatible with the standard theory prediction. Due to the large t-channel contribution, however, electroweak effects are swamped even in the backward hemisphere, where the sensitivity is still limited by statistics. Consequently the electroweak coupling constants are poorly determined, e.g. Tasso finds $g_V^{e\,2} = -0.15 \pm 0.14$ and $g_A^{e\,2} = 0.01 \pm 0.16$ or $\sin^2\theta_W = 0.28^{+0.10}_{-0.14}$. More precise data is needed to establish electroweak effects in the Bhabha scattering.

3.2. $e^+e^- \to \mu^+\mu^-$ and $e^+e^- \to \tau^+\tau^-$.

From the discussion in sec. 2 it follows that the most sensitive electroweak effect in lepton pair production appears in the forward-backward asymmetry. The measured differential cross sections[8),9)] for $e^+e^- \to \mu^+\mu^-$ and $e^+e^- \to \tau^+\tau^-$ are displayed in Figs. 2 and 3. The asymmetries, derived from a fit to the angular distributions using eqs. (1) and (6) and extrapolating the polar angle to $-1 \le \cos\theta \le +1$, are summarised in Tables 2 and 3. All data are corrected for order α^3 QED radiative effects on γ exchange diagrams[10].

The PETRA experiments on μ pair production show individually a clear deviation from QED at $\sqrt{s} = 34.5$ GeV. The combined asymmetry of $A_{\mu\mu}(34.5GeV) = (-10.8 \pm 1.1)\%$ represents a 9.8 standard deviation effect. At higher energies the magnitude of the (still preliminary)

asymmetry increases with s as expected to $A_{\mu\mu}(41.6GeV) = (-14.7 \pm 3.1)\%$, being a 4.7 st. dev. effect.

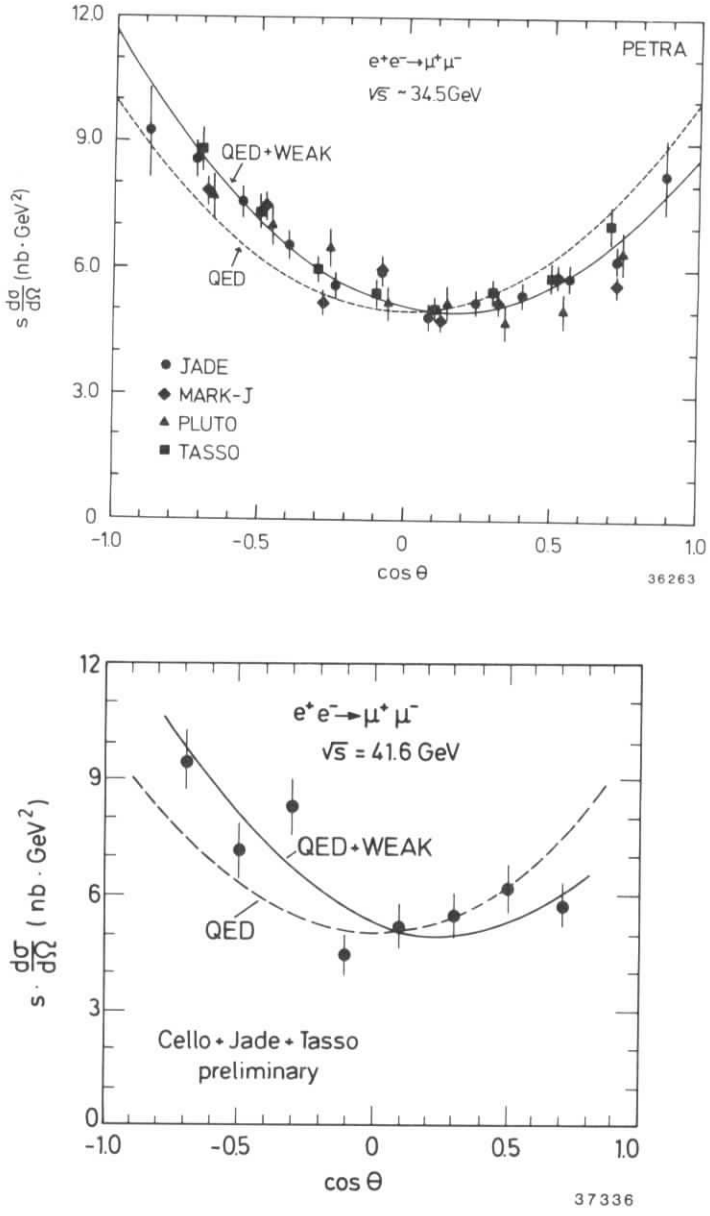

Figure 2. The differential cross section for the reaction $e^+e^- \to \mu^+\mu^-$ at a) $\sqrt{s} = 34.5\ GeV$ and b) $\sqrt{s} = 41.6\ GeV$ for PETRA experiments. The curves show fits to the respective predictions of pure QED and the electroweak theory.

τ decays are more difficult to analyse, since not all decay channels can be used and the background is more severe. Systematic uncertainties are larger and statistics are lower. The combined data on τ pair asymmetries, dominated by the Jade measurement, gives $A_{\tau\tau}(34.5GeV) = (-7.6 \pm 1.9)\%$ and constitutes the first observation of a significant electroweak interference (4 st. dev.) in the heavy lepton sector. The observed asymmetries of all experiments except Cello seem to be slightly smaller in magnitude than those for the μ pairs. However, no conclusion can be drawn on the present statistical basis.

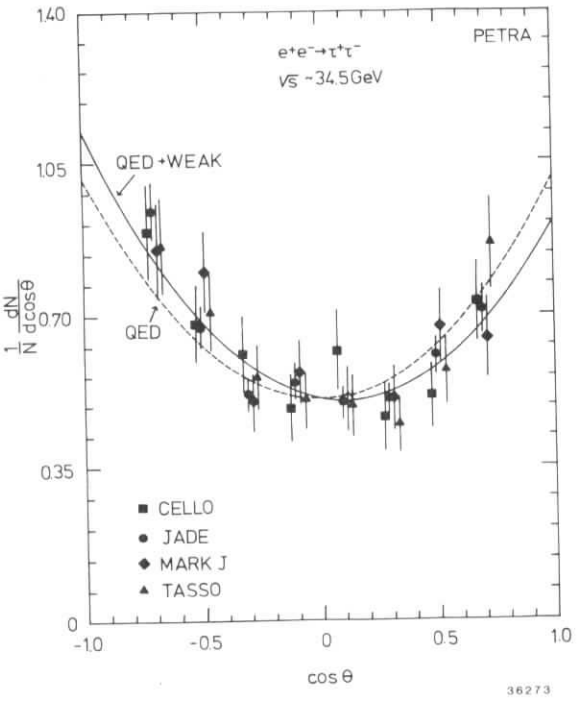

Figure 3. The differential cross section for the reaction $e^+e^- \rightarrow \tau^+\tau^-$ at $\sqrt{s} = 34.5\ GeV$ for PETRA experiments. The curves show fits to the respective predictions of pure QED and the electroweak theory.

Table 2. Results on the asymmetry in $e^+e^- \rightarrow \mu^+\mu^-$

Experiment	$\sqrt{s}\ (GeV)$	$N_{\mu\mu}$	$A_{\mu\mu}(\%)$
Cello	34.2	387	-6.4 ± 6.4
Jade	34.4	3400	$-11.0\pm1.8\pm<1$
Mark J	34.6	3658	$-11.7\pm1.7\pm<1$
Pluto	34.7	1550	$-12.4\pm3.1\pm<1$
Tasso	34.5	2673	$-9.1\pm2.3\pm0.5$
combined	34.5	11668	-10.8 ± 1.1
Cello	42.5	108	-13.4 ± 9.4
Jade	41.5	444	-14.6 ± 4.8
Mark J	41.1	480	-15.8 ± 5.3
Tasso	42.4	174	-13.1 ± 8.8
combined	41.6	1206	-14.7 ± 3.1

Table 3. Results on the asymmetry in $e^+e^- \to \tau^+\tau^-$

Experiment	$\sqrt{s}$ (GeV)	$N_{\tau\tau}$	$A_{\tau\tau}$(%)
Cello	34.2	434	-10.3 ± 5.2
Jade	34.6	1612	-7.6 ± 2.7
Mark J	34.6	860	-7.8 ± 4.0
Tasso	34.4	517	-5.4 ± 4.5
combined	34.5	3432	-7.6 ± 1.9

3.3. Radiative Corrections.

Radiative corrections are very important for all cross section measurements, since higher order diagrams also produce a forward-backward asymmetry. We want to discuss briefly their influence on the μ pair asymmetry measured at 34.5 GeV.

The radiative corrections can be split in 3 categories:

1. QED radiative corrections to graphs involving photons, e.g. vertex corrections, vacuum polarisation, external bremsstrahlung, box diagrams. These contributions have been calculated up to order α^3, they are well understood and well tested by experiments. All experiments apply these corrections, usually provided by Monte Carlo programs[10]. Depending on experimental conditions they typically contribute to the observed asymmetry a positve value of $\Delta A_{\mu\mu} = +1.5\%$.

2. QED radiative corrections to graphs involving Z^0 exchange and graphs with a photon and the Z^0. These effects have been evaluated by Monte Carlo with particular emphasis on hard photon bremsstrahlung[11]. For typical experimental selection criteria they amount to $\Delta A_{\mu\mu} = +0.7\%$.

3. Weak radiative corrections to graphs involving the Z^0, $W^\pm$, Higgs, etc... These corrections depend strongly on the renormalisation scheme used. They have been calculated by many authors[12], but only recently in a form applicable to PETRA experiments.

As an illustration we give the results of the radiative corrections calculations of different groups[12] neglecting the photonic QED contributions (i.e. point 1).

Brown et al. using α, $\sin^2\theta_W$ and m_Z as renormalisation parameters calculated the diagrams of point 3 using the results of Ref. 11) for point 2. Their result is $A_{\mu\mu}^{Born} = -8.65\%$, $A_{\mu\mu}^{rad.corr.} = -8.60\%$ or $\Delta A_{\mu\mu}^{weak} = +0.05\%$.

Böhm and Hollik using the same renormalisation parameters perform the full one loop electroweak radiative corrections resulting in $A_{\mu\mu}^{Born} = -8.65\%$, $A_{\mu\mu}^{rad.corr.} = -8.75\%$ or $\Delta A_{\mu\mu}^{weak} = -0.10\%$.

Wetzel uses α, G_F and m_Z as renormalisation constants and after full one loop calculations arrives at $A_{\mu\mu}^{Born} = -9.23\%$, $A_{\mu\mu}^{rad.corr.} = -8.63\%$ or $\Delta A_{\mu\mu}^{weak} = +0.60\%$.

Although the net corrections are quite different, the final answer, i.e. the asymmetry to be observed in the experiments, is the same due to differences already at the Born level, eq. (6). Thus the radiative corrections calculations seem to produce converging results, the differences being smaller than the present statistical and systematic uncertainties. However, one has to be aware of the renormalisation scheme used.

3.4. Conventional determination of leptonic coupling constants.

In order to interprete the data and extract the electroweak coupling constants, the theoretical lepton pair asymmetry obtained from eqs. (5) and (3b) neglecting the Z^0 width is used

$$A_{\mu\mu,\tau\tau} = \frac{3\,\rho\,G_F}{4\sqrt{2}\,\pi\,\alpha}\cdot\frac{m_Z^2\,s}{s-m_Z^2}\cdot g_A^e\,g_A^{\mu,\tau}\,. \tag{7}$$

This formulation has 3 independent parameters: ρ, G_F and m_Z. It is not very sensitive to the axact value of m_Z. Assuming the standard theory with $m_Z = 93$ GeV and applying radiative corrections the expected asymmetries are $A^{GWS}_{\mu\mu,\tau\tau}(34.5\ GeV) = -8.8\%$ and $A^{GWS}_{\mu\mu,\tau\tau}(41.6\ GeV) = -14.1\%$. The measured values are in good agreement with the standard theory, although the combined μ pair results at 34.5 GeV are about two standard deviations away. Eq. (7) can be used to measure the product of the axial vector couplings $g_A^e \cdot g_A^\mu$ and $g_A^e \cdot g_A^\tau$. The results are summarised in Table 4. From $\nu\,e$ scattering, and using the $e^+e^- \to l^+l^-$ data to single out the axial vector dominated solution, one obtains[13] for the electron axial coupling $g_A^e = -0.52 \pm 0.06$, in accord with the standard theory prediction. Inserting $g_A^e = -\frac{1}{2}$ one finds for the axial coupling of the muon $g_A^\mu = -0.58 \pm 0.05$and for the axial coupling of the tau $g_A^\tau = -0.44 \pm 0.10$. Both values are in good agreement and of comparable quality with that obtained in neutrino electron scattering. They confirm the standard theory, the grouping of leptons into lefthanded weak isospin doublets and righthanded weak isospin singlets and nicely demonstrate the concept of $e-\mu-\tau$ universality.

Table 4. Results on electroweak axial vector couplings for leptons

	$g_A^e \cdot g_A^\mu$	$g_A^e \cdot g_A^\tau$
$\sqrt{s} = 34.5 GeV$	0.295 ± 0.029	0.22 ± 0.05
$\sqrt{s} = 41.5 GeV$	0.274 ± 0.060	–
combined	0.289 ± 0.025	0.22 ± 0.05
with $g_A^e = -0.50$	$g_A^\mu = -0.58 \pm 0.05$	$g_A^\tau = -0.44 \pm 0.10$

Using both Bhabha and μ pair production data a single parameter fit within the standard theory results in $\sin^2\theta_W = 0.27 \pm 0.07$ (Tasso). This value is in good agreement with $\sin^2\theta_W = 0.215 \pm 0.04 \pm 0.015$ obtained in an also purely leptonic neutrino electron scattering experiment[14] at much lower spacelike momentum transfer.

3.5. Determination of $\sin^2\theta_W$ from lepton pair asymmetry.

The theoretical asymmetry can also be written in a slightly **different way**[2] **as**

$$A_{\mu\mu,\tau\tau} = \frac{3}{8}\frac{1}{\sin^2\theta_W\,\cos^2\theta_W}\cdot\frac{s}{s-m_Z^2}\cdot g_A^e\,g_A^{\mu,\tau}\,. \tag{8}$$

This is the original neutral current formulation, valid in general $SU(2)_L \times U(1)$ models and free from any assumption on the ρ parameter. With the $SU(2)_L$ assignment $g_A^e = g_A^\mu = g_A^\tau = -\frac{1}{2}$ there are only two free parameters, the mass m_Z of the Z^0 and the neutral current mixing angle $\sin^2\theta_W$. Eq. (8) can then be used to test the consistency with the standard theory, wherein a measurement of m_Z fixes $\sin^2\theta_W$ and vice versa. Taking radiative corrections into account the relation is[15]

$$m_Z = \frac{(38.65 \pm 0.05)\ GeV}{\sin\theta_W\,\cos\theta_W}\,. \tag{9}$$

There is a strong dependence of the asymmetry on both parameters as illustrated in Fig. 4. Plotted is the expected asymmetry as function of $\sin^2\theta_W$ with various mass values as parameters.

If one takes $m_Z = 93 \pm 2\ GeV$, the average of the UA1 and UA2 experiments[3], the asymmetry

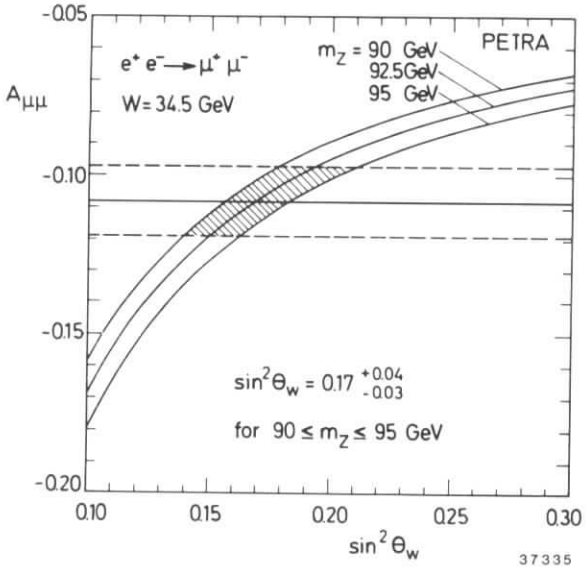

Figure 4. The expected asymmetry $A_{\mu\mu}$ as function of the weak mixing angle at $W = 34.5\ GeV$ with different m_Z values as parameters. The PETRA results are indicated by the horizontal band.

provides a very sensitive determination of $\sin^2\theta_W$. The range allowed by PETRA μ pair results for $90 \leq m_Z \leq 95\ GeV$ is shown as a shaded area and determines the neutral coupling constant to $\sin^2\theta_W = 0.17^{+0.04}_{-0.03}$. Including the 41.6 Gev data gives $\sin^2\theta_W = 0.17 \pm 0.03$. This value has to be compared with results from other experiments which cluster around $\sin^2\theta_W \sim 0.22$. It is lower by about two standard deviations reflection the larger observed μ pair asymmetry. The τ pairs, of course, are less precise yielding $\sin^2\theta_W = 0.27^{+0.10}_{-0.07}$.

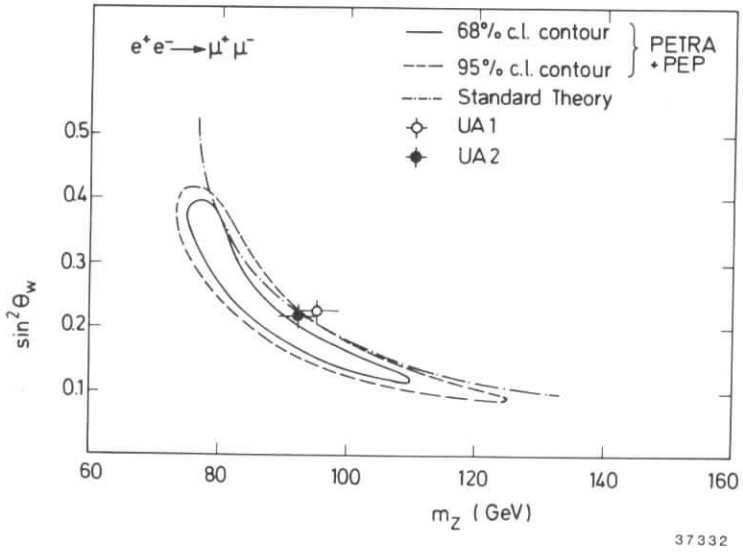

Figure 5. Contours of allowed regions of $\sin^2\theta_W$ versus m_Z derived from $e^+e^- \rightarrow \mu^+\mu^-$ results obtained at PETRA and PEP. The results from UA1 and UA2 and the standard theory prediction are shown as well.

In Fig. 5 are shown the allowed regions in the $\sin^2\theta_W - m_Z$ plane for the combined μ pair data from PETRA and PEP using the asymmetry as well as the total cross section. Shown as well are the measurements of UA1 and UA2, which just touch the 95% confidence contour. Similarly the standard theory prediction , eq. (9), is just compatible with the $e^+e^- \to \mu^+\mu^-$ results. For $m_Z = 93 \pm 2\,GeV$ the combined fit gives $\sin^2\theta_W = 0.18 \pm 0.02$.

Finally in Fig. 6 is shown the available data on $A_{\mu\mu}$ as function of the squared center of mass energy. A clear increase in absolute magnitude with s is observed in accordance with the standard theory expectations. Comparing to possible propagator effects limits the Z^0 mass to $66 < m_Z < 138\,GeV$ at 95 % $c.l.$, a value of not much interest after the Z^0 discovery. However it is illustrative to see the dependence of the expected μ pair asymmetry on $\sin^2\theta_W$.

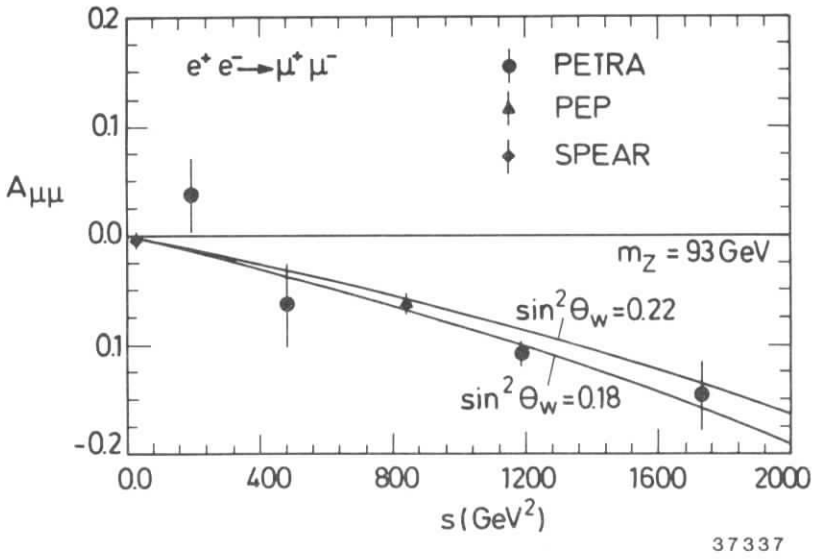

Figure 6. The measured asymmetry in $e^+e^- \to \mu^+\mu^-$ as function of the square of the c.m. energy. Data points are averages over several experiments. The curves show the dependence on 2 values of the weak mixing angle $\sin^2\theta_W$.

4. Production and decays of heavy quarks.

The heavy quarks charm and bottom are abundantly produced in e^+e^- annihilation at a rate of 4/11 and 1/11 respectively. Among the main interests are to determine their weak axial vector couplings through the expected large forward-backward asymmetries and to learn about heavy quark weak decay dynamics. Lifetime measurements[16] and fragmentation characteristics[17] will be discussed by other speakers to this conference. With existing detectors flavour tagging turns out to be quite delicate. Two methods are available, either the reconstruction of meson resonances (e.g. $D^{*\pm}$, $D^{\pm}$, $F^{\pm}$) or the analysis of inclusive lepton spectra from semileptonic charm and bottom decays. Both methods suffer from low statistics, mainly due to the small branching ratios involved and severe background problems.

4.1. D^* analysis.

The so far cleanest method of heavy flavour and in particular charm flavour tagging is to use $D^{*\pm}$ decays. At PETRA experiments the signals of $D^{\pm}$ and $F^{\pm}$ are highly background contaminated and B mesons for bottom tag have not yet been found.

Jade and Tasso[18] have searched for

$$D^{*\pm} \rightarrow D^0 \pi^{\pm}$$

with the subsequent decays

$D^0 \rightarrow K^- \pi^+$	$(br\ 2.4 \pm 0.4\ \%)$	Jade,Tasso
$D^0 \rightarrow K^- \pi^+ \pi^0$	$(br\ 9.3 \pm 2.8\ \%)$	Tasso
$D^0 \rightarrow K^- \pi^+ \pi^- \pi^+$	$(br\ 4.5 \pm 1.3\ \%)$	Tasso

to tag the c quark. No particle identification is used, but th assigned K^- mass uniquely taggs the charm flavour (and the charge conjugate decays the $\bar{c}$ quark). The trick is to cut on the the low Q value $\Delta = M(D^{*+} - M(D^0) = M(D^0\pi^+) - M(D^0) = 145\ MeV$. Due to the good resolution in Δ and the hard D^* fragmentation function a cut on $z_{D^*} = E_{D^*}/E_{beam} > 0.5$ selects an almost pure smple of c quarks with low background from B decays and other sources ($\sim 20\%$). The observed angular distribuions are shown in Fig. 7. The results of the fitted asymmetries and the extracted axial vector couplings and listed in Table 6. They are compatible with the standard theory.

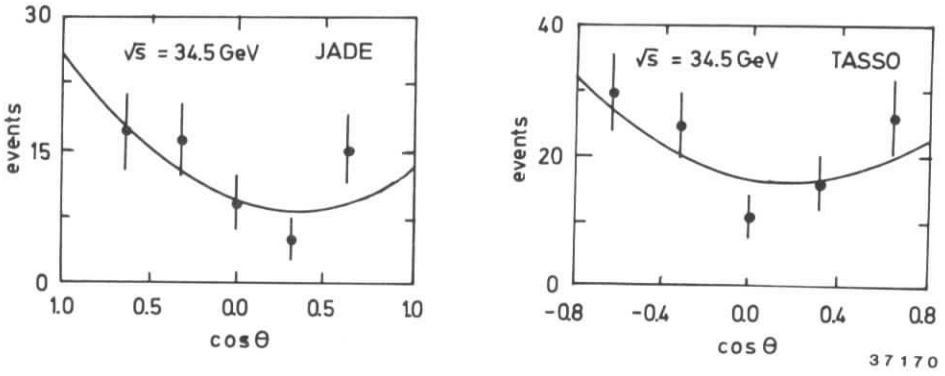

Figure 7. Angular distribution of D^* production from Jade and Tasso. Curves show the fits to the data.

Tasso has used its Cherenkov counters to identify $K^{\pm}$ mesons and set limits on $D^0\overline{D^0}$ mixing occuring via $D^{*+} \rightarrow D^0\pi^+ \rightarrow K^-\pi^+\pi^-$ and $D^{*+} \rightarrow D^0\pi^+ \rightarrow \overline{D^0}\pi^+ \rightarrow K^-\pi^+\pi^-$. Eight events of the first decay mode and none of the second reaction have been found. This gives an upper limit on the probability that a D^0 transforms into a $\overline{D^0}$ of 0.29 (90% *c.l.*).

4.2. Prompt leptons in heavy quark decays.

The prompt leptons from semileptonic decays of heavy quarks

$$b \rightarrow l^-\ \overline{\nu}_l\ X \qquad \text{and}$$
$$c \rightarrow l^+\ \nu_l\ X$$

($l = e, \mu$) provide a unique signature to identify the primary quark flavours. Large background, however, arises from cascade decays $b \rightarrow cX \rightarrow l^+\nu_l X$, u,d,s decays, $\pi^{\pm}$ and $K^{\pm}$ decays and punch through for μ identification and overlaps of $\pi^{\pm}\gamma$ and Dalitz decays for e identification. They all tend to dilute the expected asymmetry and have to be well under control.

All experiments[19] use the transverse momentum $p_{\perp}$ of the final state lepton with respect to a conveniently chosen jet axis (mostly thrust or sphericity); b quarks are supposed to produce a harder $p_{\perp}$ spectrum than c quarks. As a second discrimination parameter serve the total lepton

momentum (Cello, Tasso), event shape variables like thrust (Mark J) or the transvers jet mass (Jade). As an example Fig. 8 shows the transverse muon momentum spectrum $P_\perp^2$ of the Mark J group. In Fig 8a it is compared with the properly normalised inclusive hadron spectrum of Tasso. There is a clear excess of muons around $p_\perp^2 \sim 4\ GeV^2$, indicative for the decay of a heavy particle with a mass of about 5 GeV. In Fig. 8b the relative contributions from c and b quark decays as predicted by Monte Carlo are shown as well. They fix the semileptonic branching ratios. The $p_\perp$ spectrum is not very sensitive to the form of the fragmentation function, for

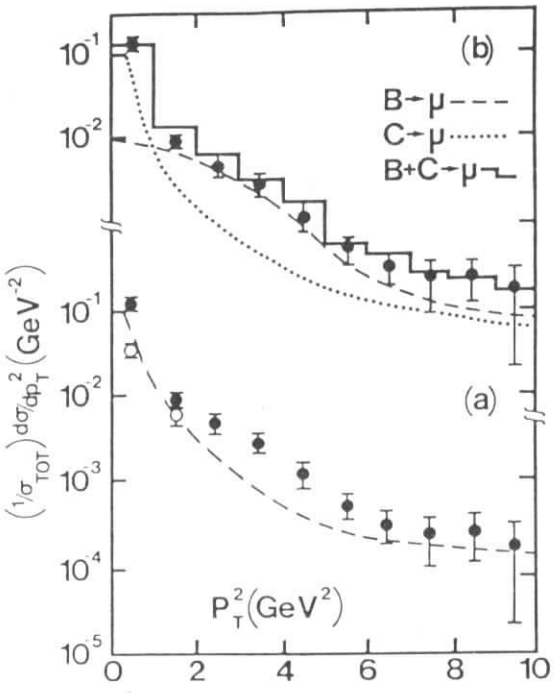

Figure 8. The $p_\perp^2$ spectrum of inclusive muons measured by Mark J. a) Comparison to the inclusive hadron spectrum from Tasso. b) Comparison of the data with the relative contributions from charm and bottom decays from Monte Carlo calculations.

which the Peterson et al.[29] type has been used. Adding both contributions and the estimated background gives a reasonable description of the data. At high $p_\perp > 1.2\ GeV$ the majority of leptons comes from B decays, whereas in the charm enriched region below $p_\perp < 1.2\ GeV$ there is a sizeable background from light quark decays.

The results for the fitted asymmetries after background correction are summarised in Tables 6 and 7 and compared to the lowest order GWS prediction. Quark mass effects, which reduce the expected asymmetries are not taken into account. The combined data using all channels from all PETRA experiments yield $A_{c\bar{c}} = -15.9 \pm 5.8\%$ for the charm quark and $A_{b\bar{b}} = -27.3 \pm 6.4\%$ for the bottom quark. Despite the higher production rate the measured charm quark asymmetry is less significant due to low statistics in D^* tagging and more severe background problems in the lepton spectrum. They are in good agreement with the standard theory prediction of $A_{c\bar{c}}^{GWS} = -14\%$ and $A_{b\bar{b}}^{GWS} = -27\%$. The present analyses, giving $g_A^c = 0.57 \pm 0.20$ and $g_A^b = -0.50 \pm 0.12$, can be considered as a first step towards a determination of the axial vector couplings of the heavy quarks. The difficult systematic uncertainties seem to be manageable, but clearly much more data, to be expected soon at higher energies, are needed to get precise values.

Table 6. Results on the charm quark asymmetry and the axial vector coupling constant

Experiment	$\sqrt{s}$ (GeV)	$A_{c\bar{c}}$ (%)	g_A^c	method
Jade	34.4	-27 ± 14	0.85 ± 0.50	D^*
Tasso	34.4	-13 ± 10	0.45 ± 0.35	D^*
Mark J	34.6	-16 ± 9	0.6 ± 0.3	$c \rightarrow \mu\nu X$
Tasso	34.6	-3 ± 20	0.1 ± 0.7	$c \rightarrow e\nu X$
combined	34.5	-15.9 ± 5.8	0.57 ± 0.20	
GWS theory	34.5	-14	$+0.50$	

Table 7. Results on the bottom quark asymmetry and the axial vector coupling constant

Experiment	$\sqrt{s}$ (GeV)	$A_{b\bar{b}}$ (%)	g_A^b	method
Cello	34	-43 ± 31	-0.8 ± 0.6	$b \rightarrow \mu\nu X$
		-38 ± 21	-0.7 ± 0.4	$b \rightarrow e\nu X$
Jade	34.4	-26.2 ± 8.2	-0.50 ± 0.15	$b \rightarrow \mu\nu X$
Mark J	34.6	-21 ± 19	-0.4 ± 0.4	$b \rightarrow \mu\nu X$
Tasso	34.5	-18 ± 23	-0.3 ± 0.4	$b \rightarrow \mu\nu X$
		-37 ± 28	-0.7 ± 0.5	$b \rightarrow e\nu X$
combined	34.5	-27.3 ± 6.4	-0.50 ± 0.12	
GWS theory	34.5	-27	-0.50	

The extracted semileptonic branching ratios of c and b quarks are compiled in Table 8. They represent a mixture of charged and neutral meson decays, which are supposed to be different, and still poorly known baryon decays. The electronic and muonic modes are the same within errors. The results averaged over lepton flavours are $br(c \rightarrow lX) = 10.3 \pm 1.4\%$ and $br(b \rightarrow lX) = 10.7 \pm 1.5\%$. They are in good agreement with recent measurements at PEP[20] ($br(c \rightarrow lX) = 8.4 \pm 0.7\%$) and CESR[21] ($br(b \rightarrow lX) = 11.7 \pm 0.6\%$). Simple considerations based on the spectator model and accounting for phase space and colour factors predict for heavy quark weak decays, e.g. for the bottom quark, a semileptonic branching ratio into electrons or muons of $br(b \rightarrow lX) \sim 12 - 17$ %. Non spectator contributions and QCD corrections are expected to reduce this numbers to $br(b \rightarrow lX) \sim 11 - 13$ %.

Table 8. Semileptonic branching ratios for charm and bottom quark decays

Experiment	$br\ (c \rightarrow e\nu X)$ (%)	$br\ (c \rightarrow \mu\nu X)$ (%)	$br\ (b \rightarrow e\nu X)$ (%)	$br\ (b \rightarrow \mu\nu X)$ (%)
Cello	–	$12.3 \pm 2.9 \pm 3.9$	$14.1 \pm 5.8 \pm 3.0$	$8.8 \pm 3.4 \pm 3.5$
Mark J	–	$11.5 \pm 1.5 \pm 1.3$	–	$10.5 \pm 1.5 \pm 1.3$
Tasso	$8.4 \pm 2.6 \pm 4.0$	$8.2 \pm 1.2\ ^{+2}_{-1}$	$11.9 \pm 4.9 \pm 4.0$	$11.7 \pm 2.8 \pm 1$
combined	8.4 ± 4.8	10.5 ± 1.5	13.0 ± 4.5	10.6 ± 1.6

The data have also been used to search for events with two leptons, which may occur in decays mediated by flavour changing neutral currents. From the absence of such events upper limits (95% *c.l.*) can be derived for the b quark of $br(b \rightarrow \mu^+\mu^- X) < 0.7\%$ (Jade and Mark J) and $< 2\%$ (Tasso) and for the c quark of $br(c \rightarrow \mu^+\mu^- X) < 0.7\%$ (Tasso). Topless models

predicting $br(b \to \mu^+\mu^- X) \sim 2\%$ are at variance with the data, which favour the standard classification that the b quark is a member of a weak isospin doublet. Thus, on the basis of this data the top quark should exist.

5. Weak charged currents in τ decays.

5.1. Topological branching ratios.

The topological branching ratios of τ decays $B_i = br(\tau \to$ i charged particles + neutrals) with i = 1,3,5, have been subject to dramatic changes within the last two years, well beyond the quoted errors. New data are available from Cello[22] ($\sqrt{s} = 14$ and 22 GeV) and Tasso[23] ($\sqrt{s} = 34.5$ GeV, preliminary). Both groups make extensive use of their particle identification capabilities provided by liquid argon calorimeters, electromagnetic shower counters and muon chamber systems. All decay chanels with 1-1, 1-3, 3-3 and 1-5 charged final state topologies have been investigated except e^+e^- and $\mu^+\mu^-$ pairs. Involved matrix procedures to unfold the feed through from various categories have been investigated. Decays into 5 charged particles were not observed giving upper limits of $B_5 < 0.7\%$ (95% *c.l.*) for both experiments. The topological branching ratios of Cello, $B_1 = (85.1 \pm 1.9 \pm 1.3)\%$ and $B_3 = (14.7 \pm 1.5 \pm 1.3)\%$, and Tasso $B_1 = (83.9 \pm 1.1 \pm 2.2)\%$ and $B_3 = (16.1 \pm 1.1 \pm 2.2)\%$, are compatible with each other and confirm earlier results of Cello[22] and Mark II[24].

5.2. Semihadronic branching ratios.

In order to check whether the exclusive decays sum up to the observed topological branching ratios the Cello group[22] has contributed new results on semileptonic decays of the type

$$\begin{aligned} &\tau^- \to \pi^- \, n\pi^0 \, \nu \qquad (n = 1, 2, 3) \\ &\tau^- \to \pi^- \, \pi^- \, \pi^+ \, n\pi^0 \, \nu \qquad (n = 0, 1,) \\ &\tau^- \to \pi^- \, \pi^- \, \pi^- \, \pi^+ \, \pi^+ \, \nu \, . \end{aligned}$$

Final states with up to 5 photons with $E_\gamma > 100\ MeV$ have been searched for. To fight the background from bremsstrahlung, hadron interactions in the calorimeter and overlaps, photons were required to be separated by more than 8^0 in space from charged tracks. If 2 or 3 (4 or 5) photons were present at least 1 (2) $\gamma\gamma$ combination(s) had to fit the π^0 hypothesis. These cleaning cuts reduce the overall efficiency to 37% for 2 charged prongs and 49% for multiprongs. A complete efficiency matrix to handle the various feed throughs has been built up with Monte Carlo programs. Resonance fits like $\rho^\pm \to \pi^\pm\pi^0$ have been performed to disentangle nonresonant contributions. Corrections for unidentified $\tau \to K\nu$ and $\tau \to K^*\nu$ were taken from other experiments[24]. It is worth noting that the results are independent of any assumption on the QED τ pair cross section.

A complete list of all τ branching ratios as measured by the Cello collaboration complemented with som recent results on K decays[25] are given in Table 9. First measurements of τ decays into 4 charged pions in two different charge conjugate modes are reported, offering a new test of the CVC hypothesis. The Cello results on known channels agree with those obtained by other experiments, however the numbers for some decay modes have been improved considerably. Note that the sum of all branching ratios now saturate within errors the full τ width. This is a big step forward in understanding the properties of the τ. The experimental data are in very good agreement with the predictions for a sequential heavy lepton based on the standard V-A theory[26] including the CVC (describing τ decays into an even number of pions) and PCAC (describing τ decays into an odd number of pions) hypotheses.

Table 9. τ branching ratios as measured by Cello and Delco (K final states)

decay mode	meas. br (%)	theory br (%)
$e\nu\nu$	$18.3 \pm 2.4 \pm 1.9$	18.3
$\mu\nu\nu$	$17.6 \pm 2.6 \pm 2.1$	17.9
$\rho\nu$	$22.1 \pm 1.9 \pm 1.6$	22.3
$\pi\pi^0\nu$ (non res.)	$17.6 \pm 2.6 \pm 2.1$	small
$\pi\pi\pi\pi^0\nu$	$6.2 \pm 2.3 \pm 1.7$	6.6
$\pi\pi^0\pi^0\pi^0\nu$	$3.0 \pm 2.2 \pm 1.5$	1.1
$\pi\nu$	$9.9 \pm 1.7 \pm 1.3$	10.8
$\pi\pi\pi\nu$	$9.7 \pm 2.0 \pm 1.3$	< 18.7
$\pi\pi^0\pi^0\nu$	$6.0 \pm 3.0 \pm 1.8$	"
$\pi\pi\pi\pi\pi\nu$	< 0.9	0.9
$K\nu$	0.59 ± 0.18	0.5
$Kn\pi^0\nu$	1.71 ± 0.29	1.5
$\sum$ *all*	95.4 ± 6.5	100

5.3. τ lifetime.

The τ lifetime measurement is the best method to determine the τ weak charged coupling constant G_τ

$$\Gamma_\tau = \frac{G_\tau^2 \, m_\tau^5}{192 \, \pi^3} \, . \tag{10}$$

It is related to the μ decay through

$$\begin{aligned} \tau_\tau &= \tau_\mu \left(\frac{m_\mu}{m_\tau}\right)^5 \cdot B_e(\tau \to e\nu_e\nu_\tau) \\ &= (\, 2.8 \, \pm \, 0.2 \,) \cdot 10^{-13} \; sec \, . \end{aligned} \tag{11}$$

A new measurement by the Tasso collaboration[27] using the recently installed vertex detector is available. The data were taken during an energy scan between $\sqrt{s} = 39.8$ and 45.2 GeV, with $< \sqrt{s} > = 42.5$ GeV and an integrated luminosity of 10.2 pb^{-1}. Two methods with different systematic uncertainties were investigated. The first method uses the 1-3 and 3-3 charged track topologies and measures the distance between the interaction point and the 3-prong decay vertex. The final sample consists of 50 3-track vertices. The second method measures the distance between two vertices of an event with a 3-3 charged track topology. Due to the small statistics (7 events), however, this serves only as cross check.

The vertex detector consists of a thin Be beam pipe ($0.5\% \, X_0$) at a radius of 6.5 cm, two sets of each 4 cylindrical drift chamber layers at average radii of 9.1 cm and 13.9 cm operating with a 95% A / 5% CO_2 gas mixture at 3 bar (total of $\sim 0.6\% \, X_0$) and an outer aluminum vessel at a radius of 16.0 cm ($1.7\% \, X_0$). The drift length varies between 3.5 and 4.5 mm and the average resolution achieved in the xy plane perpendicular to the beam is $\sigma_{xy} = 90 - 100 \; \mu m$. The vertex chamber is followed by a proportional chamber ($\sigma_{xy} \simeq 500 \; \mu m$) and the central drift chamber ($\sigma_{xy} \simeq 180 \; \mu m$) measuring the track length over 90 cm. All three detector elements were used in three dimensional track and vertex fitting; the multiple scattering was assumed to occur at a fixed radius around 16 cm with an average scattering angle increased by 30%. The relative alignment of the vertex detector with respect to the drift chamber is known to within 0.1 mrad in azimuth and 100 μm in x and y.

The beam spot was determined on a run-by-run basis with at least 50 tracks from different events. The typical uncertainty in x and y was 150 μm which had to be convoluted with the

beam size of $\Delta x \simeq 500\ \mu m$ and $\Delta y \simeq 10\ \mu m$ as given by the beam optics. The constructed error matrices including all correlations for track and vertex fitting have been carefullly checked with data and Monte Carlo. The decay length l_{xy} projected into the xy plane, where the resolution is best, was measured. The total decay length l was then obtained by using the z component of the momentum vector formed by the 3 tracks from the τ decay.

The error distribution of the decay length is shown in Figure 9. It peaks around 1100 μm with a mean of 1400 μm. A cut at 2500 μm removed badly reconstructed vertices. The decay length distribution of τ decays is shown in Figure 10. The center has a clear shift away from zero, the mean being $< l >= 1051 \pm 270\ \mu m$. It is not a symmetric distribution, reflecting the exponential decay folded with a gaussian resolution function. The final analysis was carried out using a maximum likelihood method. The result of the fit gives $< l >= 1082\ ^{+205}_{-261}\ \mu m$ as best estimate for the τ decay path. From the second method, measuring the distance between two vertices in 3-3 topologies, a consistent result of $< 2l >= 3200\ ^{+1100}_{-1600}\ \mu m$ or $< l >= 1600\ ^{+550}_{-800}\ \mu m$ has been obtained.

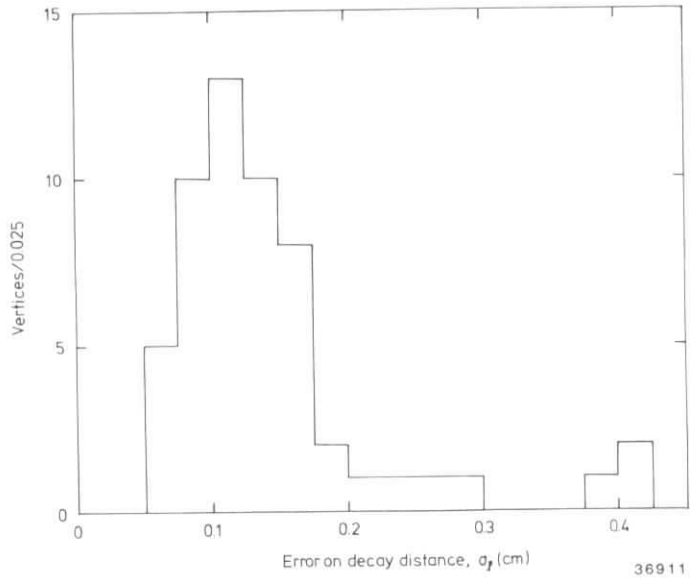

Figure 9. Error distribution of the decay distance for $\tau \rightarrow 3$ charged tracks from Tasso.

Detailed investigations of systematic uncertainties in position measurements, error matrix computation, analysis procedures, etc. with data and Monte Carlo have been performed. Selecting τ like configurations within multihadron events lead to $< l >= 54 \pm 120\ \mu m$, compatible with no bias. Similarly, Monte Carlo simulations with different decay lengths reproduced the input values. Various cross checks with the data set split in different time periods or geometrical detector acceptances, smearing the chamber or vertex positions by 2 st. dev., - all trials left the results unchanged within 10%. The overall systematic error contributing to the decay length was estimated to be 190 μm.

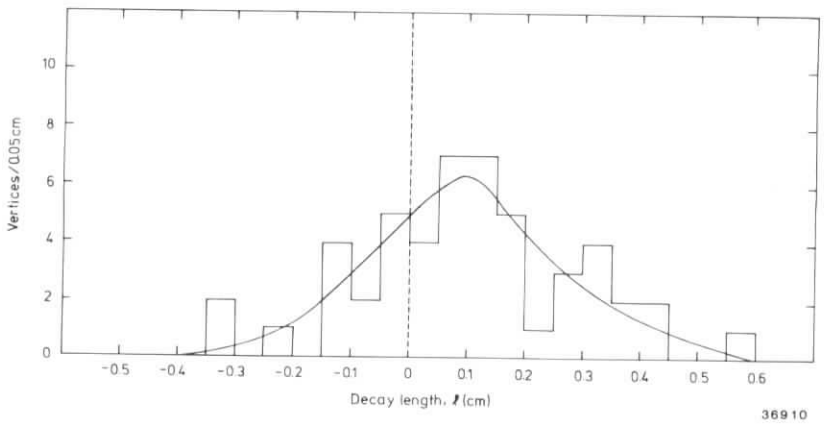

Figure 10. Decay distance distribution for $\tau \rightarrow 3$ charged tracks from Tasso. Curve shows the best fit to the data.

After correcting for initial state photon radiation, on average $\sim 7\%$ loss in the mean τ energy, the result for the τ lifetime is

$$\tau_\tau = \left(3.18 \, ^{+0.59}_{-0.75} \pm 0.56 \right) \cdot 10^{-13} \; sec \; .$$

This result confirms earlier measurements[16),28)] at PEP. It is in very good agreement with the theoretical expectation of eq. (11) based on $\mu - \tau$ universality. The charged weak coupling constant of the tau, G_τ, is within $\sim 10\%$ the same as that of the muon

$$G_\tau = \left(0.94 \, ^{+0.12}_{-0.09} \pm 0.09 \right) \cdot G_\mu \; .$$

It is a remarkable succes of τ research that within less than a decade since its discovery almost all properties of the τ have been unvealed and fit into the theoretical picture of a sequential heavy lepton. The only piece missing is a direct observation of the τ neutrino ν_τ.

Acknowledgements. I would like to thank my colleagues from the PETRA collaborations for providing and discussing new data prior to publication. In particular I acknowledge many usefull conversations with A. Böhm, B. Naroska and Ch. Youngman. It is a pleasure to thank B. Panvini for the invitation and the pleasant and stimulating atmosphere he provided at the 1984 Vanderbilt Symposium.

References.

1. S.L.Glashow, Nucl.Phys. 22 (1961) 579;
   A.Salam, Proc. eighth Nobel Symp., p.367 (ed.N.Svartholm, Stockholm, Almquist and Wiksell 1968)
   S.Weinberg, Phys.Rev.Lett. 19 (1967) 1264.

2. For a recent review see
   B.Naroska, 1983 Int. Symp. on Lepton and Photon Interactions, Ithaca, p. 96;
   A.Böhm, 1984 Rencontre de Moriond and RWTH Aachen preprints PITHA 84/11 and 84/13.
   M.Davier, XXI Int. Conf. High Energy Physics, Paris 1982, J.Phys.(Paris) Suppl. 43 (1982) C3-471.

3. UA1 Coll., G.Arnison et al., Phys.Lett. 122B (1983) 103 and Phys.Lett. 126B (1983) 398;
   UA2 Coll., G.Banner et al., Phys.Lett. 122B (1983) 476 and P.Bagnaia et al., Phys.Lett. 129B (1983) 130.

4. R.Budny, Phys.Lett. 55B (1975) 227.

5. Jade Coll., W.Bartel et al., Phys.Lett. 101B (1981) 361 and private communication;
   Mark J Coll., D.P.Barber et al., Phys.Rev.Lett. 46 (1981) 1663 and B.Adeva et al., MIT-LNS Report 128 (1983);
   Tasso Coll., M.Althoff et al., Phys.Lett. 110B (1982) 173 and Phys.Lett. 138b (1984) 441.

6. Cello Coll., H.-J.Behrend et al., Z.Phys. C16 (1983) 301;
   Jade Coll., W.Bartel et al., Z.Phys. C19 (1983) 197;
   Mark J Coll., B.Adeva et al., Phys.Rev.Lett. 48 (1982) 1701 and MIT-LNS Report 128 (1983);
   Tasso Coll., M.Althoff et al., Z.Phys. C22 (1984) 13.

7. F.A.Berends et al., Nucl.Phys. B63 (1973) 381 and Nucl.Phys. B68 (1974) 541; F.A. Berends, G.J.Komen, Phys.Lett. 63B (1976) 432; F.A.Berends, R.Kleiss, Inst. Lorentz, Leiden, preprint, July 1983.

8. Cello Coll., H.-J.Behrend et al., Z.Phys. C14 (1982) 283;
   Jade Coll., W.Bartel et al., Phys.Lett. 108B (1982) 140;
   Mark J Coll., B.Adeva et al., Phys.Rev.Lett. 48 (1982) 1701 and MIT-LNS Report 128 (1983);
   Pluto Coll., Ch.Berger et al., Z.Phys. C14 (1982) 283;
   Tasso Coll., R.Brandelik et al., Phys.Lett. 110B (1982) 173 and M.Althoff et al., Z.Phys. C22 (1984) 13.

9. Cello Coll., H.-J.Behrend et al., Phys. Lett. 114B (1982) 292;
   Jade Coll., W.Bartel et al., Phys.Lett. 108B (1982) 140;
   Mark J Coll., B.Adeva et al., Phys.Rev.Lett. 48 (1982) 1701 and MIT-LNS Report 128 (1983);
   Tasso Coll., R.Brandelik et al., Phys.Lett. 110B (1982) 173 and private communication.

10. F.A.Berends et al., Nucl.Phys. B63 (1973) 381 and Nucl.Phys. B177 (1981) 237; F.A. Berends, R.Kleiss, DESY Report 80-66 (1980).

11. F.A.Berends, R.Kleiss, S.Jadach, Nucl.Phys. B202 (1982) 63.

12. G.Passarino, M.Veltman, Nucl.Phys. B160 (1979) 151;
    G.Passarino, Nucl.Phys. B204 (1982) 237;
    M.Greco et al., Nucl.Phys. B171 (1979) 118 and Nucl.Phys. B197 (1982) 543;
    R.W.Brown, R.Decker, E.A.Paschos, Phys.Rev.Lett. 52 (1984) 1192;
    M.Böhm, W.Hollik, Nucl.Phys. B204 (1982) 45 and DESY Report 83-060 (1983);
    W.Wetzel, Heidelberg University preprint, May 1983.

13. Recent compilations of electroweak parameters can be found in
J.E.Kim et al., Rev.Mod.Phys. 53 (1981) 211;
Particle Data Group, Phys.Lett. 112B (1982) 1;
W.Krenz, RWTH Aachen preprint, Pitha 82/26 (1982).

14. F.Bergman et al., Phys.Lett. 117B (1982) 272;

15. W.J.Marciano, 1983 Int. Symp. on Lepton and Photon Interactions, Ithaca, p. 96

16. L.Gardney, Contribution to this conference

17. W.Hoffman, J.v.Krogh, Contributions to this conference

18. Tasso Coll., M.Althoff et al., Phys.Lett. 126B (1983) 493, Phys.Lett. 138B (1984) 318 and private communication.
Jade Coll., private communication

19. Cello Coll., H.-J.Behrend et al., Z.Phys. C19 (1983) 291;
Jade Coll., W.Bartel et al., Phys.Lett. 132B (1983) 241 and private communication:
Mark J Coll., B.Adeva et al., Phys.Rev.Lett. 51 (1983) 443 and MIT-LNS Report 128 (1983);
Tasso Coll., M.Althoff et al., Z.Phys. C22 (1984) 219 and private communication.

20. M.Sakuda, Contribution to this conference

21. K.Kinoshita, Contribution to this conference

22. Cello Coll., H.-J.Behrend et al., Z.Phys. C23 (1984) 103 and Phys.Lett. 127B (1983) 270.

23. Tasso Coll., private communication;

24. Mark II Coll., J.M.Dorfan et al., Phys. Rev. Lett. 46 (1981) 215, G.S.Abrams et al., Phys. Rev. Lett. 48 (1982) 1586, C.A.Blocker et al., Phys. Rev. Lett. 49 (1982) 1369 and Phys.Lett. 109B (1982) 119.

25. Delco Coll., G.B.Mills et al., preprint CALT-68-1104 (1984).

26. H.B.Thacker, J.J.Sakurai, Phys.Lett. 36B (1971) 162;
Y.S.Tsai, Phys.Rev. D4 (1971) 2821;
F.J.Gilman, D.H.Miller, Phys.Rev. D17 (1978) 1846;
N.Kawamato, A.I.Sanda, Phys.Lett. 76B (1978) 446;
T.N.Pham et al., Phys.Lett. 78B (1978) 623.

27. Tasso Coll., M.Althoff et al., DESY 84-017 (1984).

28. Mark II Coll., J.A.Jaros et al., Phys.Rev.Lett. 51 (1983) 955.

29. C.Peterson et al., Phys.Rev. D27 (1983) 105.
Y.S.Tsai, Phys.Rev. D4 (1971) 2821;